Manuscript submitted to
AIMS' Journals
Volume **X**, Number **0X**, XX **200X**

Website: http://AIMsciences.org

pp. **X–XX**

ASYMPTOTICS OF BLOWUP SOLUTIONS FOR THE AGGREGATION EQUATION

Yanghong Huang

Department of Mathematics, Simon Fraser University, 8888 University Dr.
Burnaby, BC V5A 1S6, Canada

Andrea Bertozzi

520 Portola Plaza, Math Sciences Building 6363
Los Angeles, CA 90095, USA

Abstract. We consider the asymptotic behavior of radially symmetric solutions of the aggregation equation $u_t = \nabla \cdot (u \nabla K * u)$ in $\mathbb{R}^n$, for homogeneous potentials $K(x) = |x|^\gamma$, $\gamma > 0$. For $\gamma > 2$, the aggregation happens in infinite time and exhibits a concentration of mass along a collapsing δ-ring. We develop an asymptotic theory for the approach to this singular solution. For $\gamma < 2$, the solution blows up in finite time and we present careful numerics of second type similarity solutions for all γ in this range, including additional asymptotic behaviors in the limits $\gamma \to 0^+$ and $\gamma \to 2^-$.

1. **Introduction.** This paper is devoted to the asymptotic behavior of radially symmetric blowup solutions to the aggregation equation

$$u_t = \nabla \cdot (u \nabla K * u) \quad \text{in } \mathbb{R}^n, \tag{1}$$

where u is the mass density and $K * u$ is the convolution of u with some kernel K.

This equation arises in a number of models in physics and biology. In the Keller-Segel model [23] of chemotaxis in bacteria, the kernel associated with the convection of the bacteria density is the Newtonian potential $K(x) \sim |x|^{2-n}$. In the community of granular flow [3, 32], the kernel $K(x) = |x|^3/3$ is used in the kinetic equation for the velocity distribution function u of the granular medium. Recently, the attractive-repulsive kernel

$$K(x) = FLe^{-|x|/L} - e^{-|x|}$$

is used extensively to model animal swarming behavior [14, 16, 27, 29], where F and L are parameters controlling the strength and characteristic length of the attraction.

Besides these kernels from different physical and biological settings, the mathematical theory of this equation with various general kernels as well with diffusion effects has also been studied thoroughly in the past few years [9, 10, 11, 26, 30, 31]. The special case in one dimension with degenerate diffusion is investigated by Burger, Capasso, and Morale [10], and Burger and Di Francesco [10]. The inviscid case in one dimension is studied in [9, 18, 19], mainly for kernels of the form

2000 *Mathematics Subject Classification.* Primary: 35B40, 35B44; Secondary: 92D50.

Key words and phrases. Aggregation equation, blowup, asymptotic behavior, self-similar solutions.

$K(x) = -e^{-|x|}$. The corresponding theory in higher dimensions is studied by Laurent [24] and Bertozzi and Laurent [7] in classical Sobolev spaces, and by Bertozzi and Brandman [4] in L^∞ spaces. Local vs. global well-posedness for this problem is shown to be distinguished by a sharp condition on the kernel [5], namely an Osgood condition involving unboundedness of $\int 1/K'(r)dr$ near the origin. For power-law kernels $K(x) = |x|^\gamma$, this translates into $\gamma = 2$ being the critical power distinguishing finite time vs. infinite time blowup. Earlier work [21] by the authors focuses on the special case $\gamma = 1$, showing numerical evidence of second-kind self-similar blowup in all dimensions. This blowup solution remains in some L^p spaces at the blowup time, which motivated the work [8] to study its well-posedness in general L^p spaces. The aggregation equation (1) can also be regarded as the continuum limit of the discrete system [5, 9, 10, 18, 19, 28] for L particles located at $\{x_1, x_2, \cdots, x_L\}$ with mass $\{m_1, m_2, \cdots, m_L\}$, whose governing ODEs are

$$\frac{d}{dt}x_i(t) = -\sum_{j\neq i} m_j \nabla K(x_j - x_i), \quad i = 1, 2, \cdots, L. \tag{2}$$

This particle system (2) converges to the continuous equation (1) under different conditions [9, 10, 28], and the notion is weak measure-valued solutions is introduced inẽqrefmartin08. The complete theory of these weak measure-valued solutions is developed in [13], based on the underlying gradient flow structure in the space of probability measures [1] and other techniques from optimal transport [33], unifying the treatment of the discrete particle system and its continuous limit.

Inspired by the blowup profiles studied in this paper, new theoretical work [6] shows the existence of measure solutions for more singular kernels in the case of radially symmetric data and proves existence of monotone decreasing measure solutions for power law kernels with $2 - n \leq \gamma < 2$, including the case of the Newtonian potential, providing some directions to continue the solutions after blowup.

Of particular interest in this equation is the blowup of smooth or bounded solutions to (1). In one dimension, the same equation with $K(x) = |x|^\gamma/\gamma$, i.e.

$$\frac{\partial u(v,t)}{\partial t} = \frac{\partial}{\partial v}\left[u(v,t)\int_{\mathbb{R}} |v-w|^{\gamma-2}(v-w)u(w,t)dw\right],$$

is well studied as one of the kinetic models in granular flow [32, 3], where $u(v,t)$ is the velocity distribution function of the granular medium. The long time asymptotic behavior of the solution is studied first for the special case $\gamma = 3$ in [12] and for general case $\gamma > 1$ in [25].

In this paper, we study various asymptotics of the blowup solutions for the homogeneous kernel $K(x) = |x|^\gamma$ in higher dimensions. The choice of this kernel is for convenience of analysis and similar behaviors are expected for general kernels with leading order $|x|^\gamma$ near the origin. For the special case $\gamma = 2$, thanks to conservation of mass and center of mass, the exact solution can be computed explicitly as

$$u(x,t) = e^{2nMt}u_0(e^{Mt}x),$$

where $u_0(x)$ is the initial condition at time $t = 0$ and $M = \int u(x)dx$ is the total mass.

When $\gamma \in (2,\infty)$, the solutions exist for any smooth initial data and the only possible blowup is at infinite time [5]. The long time behavior of this blowup process is investigated by introducing a similarity transform, followed by a detailed analysis of the transformed equation in similarity variables in Section 2. When $\gamma \in (0,2)$, the solutions exist only on finite time intervals [5]. The dynamics of these blowup solutions for the special case $\gamma = 1$ is studied by the authors in [21]. What is interesting about these self-similar blowup solutions is their anomalous scaling. We show in this paper that the same behavior occurs for all $\gamma \in (0, 2)$ in Section 3. We also consider the asymptotic behavior of the solution for $\gamma \to 0^+$ and $\gamma \to 2^-$. Some conclusions and open problems are presented on Section 4.

2. Long time Asymptotics for $\gamma > 2$.

The blowup mechanism of the solutions to (1) is ultimately related to the underlying system of ODEs [4] for individual particles. For compactly supported or fast decaying initial data, this mechanism is determined by the singularity of the kernel near the origin, or equivalently the speed of the collapse of the particle system (2). For the homogeneous kernel $K(x) = |x|^\gamma$, the larger γ, the slower the speed when two particles collide. This blowup/non-blowup behavior is analyzed rigorously by a generalization of the Osgood condition for ODEs in [5]. In particular, when $\gamma > 2$ the solution blows up only at infinite time. In this section we first examine the long time limit of the solutions after a similarity transformation. Then we consider the special case of a radially symmetric solution for more detailed asymptotics of the infinite time blowup.

2.1. Convergence of general solutions.

In this subsection, we will study the long time asymptotics of the solutions to (1). A convenient way to do this is via the *similarity variables*:

$$y = xt^\beta, \quad \tau = \ln t, \quad U = t^{-\alpha} u \tag{3}$$

or $u(x, t) = t^\alpha U(xt^\beta, \tau)$. The new function U satisfies the equation

$$U_\tau = \nabla \cdot [U(\nabla K * U - \beta y)] \tag{4}$$

provided that

$$\alpha = \frac{n}{\gamma - 2}, \qquad \beta = \frac{1}{\gamma - 2}. \tag{5}$$

These exponents α and β are determined uniquely by the condition of no explicit dependence of (4) in τ and the conservation of mass for U. Such scaling is appropriate for infinite time singularity when $\gamma > 2$ but not for finite time singularity when $\gamma < 2$ as considered later. We note that both the original equation (1) and the transformed equation (4) converse mass, and center of mass (assumed to be at the origin).

The long time behavior of the solution U can be deduced from the associated Lyapunov function, or the energy

$$E(U) = \frac{1}{2}\int_{\mathbb{R}^n}\int_{\mathbb{R}^n} K(y - z)U(y)U(z)dydz - \frac{\beta}{2}\int_{\mathbb{R}^n} |y|^2 U(y)dy. \tag{6}$$

In fact, the dynamics (4) can be regarded as a gradient flow of this energy in the space of probability measures [33, 1], i.e.

$$\frac{\partial U}{\partial \tau} = -\text{div}\left[U\left(\frac{\delta E}{\delta U}\right)\right] \tag{7}$$

and

$$\frac{d}{d\tau}E(U) = -\int_{\mathbb{R}^n} U(y)|\nabla K * U(y) - \beta y|^2 dy \le 0, \tag{8}$$

where $\frac{\delta E}{\delta U}$ is the Fréchet derivative of the energy E with respect to U.

To include all the limiting solutions of U, possibly Dirac-delta functions, in the solution space, we introduce the space of measures with center of mass at the origin,

$$\mathcal{M} = \left\{ \mu \text{ is a non-negative Radon measure on } \mathbb{R}^n, \mu(\mathbb{R}^n) = M, \int_{\mathbb{R}^n} y d\mu = 0 \right\},$$

and the space of measures with bounded γ-th order moment,

$$\mathcal{P}_\gamma(\mathbb{R}^n) = \left\{ \mu \in \mathcal{M} : \int_{\mathbb{R}^n} |y|^\gamma d\mu < \infty \right\}.$$

By abuse of notation, we write $U(x)dx$ instead of $d\mu$ in the following. For any initial condition $U(\cdot, 0) \in \mathcal{P}_\gamma(\mathbb{R}^n)$, we can show that the γ-th order and thus the second order moments are bounded uniformly when τ goes to infinity. In fact,

$$\begin{aligned}\int |y|^2 U(x)dx &= \frac{1}{2M} \int (|y|^2 + |z|^2 - 2y \cdot z) U(y) U(z) dydz \\ &= \frac{1}{2M} \iint |y - z|^2 U(y) U(z) dydz\end{aligned}$$

Using the Hölder's inequality

$$\iint |y - z|^2 U(y) U(z) dydz \leq \left(\iint |y - z|^\gamma U(y) U(z) dydz \right)^{2/\gamma} M^{2-4/\gamma},$$

we have

$$\begin{aligned}E(U) &= \frac{1}{2} \iint |y - z|^\gamma U(y) U(z) dydz - \frac{\beta}{4M} \iint |y - z|^2 U(y) U(z) dydz \\ &\geq \frac{M^{2-\gamma}}{2} \left(\iint |x - y|^2 U(x) U(y) dxdy \right)^{\gamma/2} - \frac{\beta}{4M} \iint |x - y|^2 U(x) U(y) dxdy\end{aligned}$$

Since $\gamma > 2$, $E(U)$ is bounded below on $\mathcal{P}_\gamma(\mathbb{R}^n)$ and the second moments (similarly the γ-th order moments) of U are bounded above. Consequently, the boundness of these moments implies the tightness and therefore the weak compactness of the sequence of solutions $U(\tau)$ in $\mathcal{P}_\gamma(\mathbb{R}^n)$. This proves the following theorem:

Theorem 2.1. *Let $U(\tau)$ be the solution to the equation (4) in $\mathcal{P}_\gamma(\mathbb{R}^n)$. Then along a subsequence $\{\tau_k\}$, the functions $\{U(\tau_k)\}$ have a limit in $\mathcal{P}_\gamma(\mathbb{R}^n)$ when τ_k goes to infinity, which is denoted as U_∞.*

We remark that the above argument does not work for the case $\gamma < 2$, in which E is not bounded below. In fact, as first shown numerically in [21] and generalized later in this paper, the self-similar solutions are of the second kind and it is not possible to introduce any exact similarity variables as (3).

Since $E(U)$ is bounded below, from the dissipation inequality (8), any limiting measure U_∞ must satisfy the equilibrium condition

$$\int_{\mathbb{R}^n} U_\infty(y) |\nabla K * U_\infty(y) - \beta y|^2 dy = 0. \tag{9}$$

In other words, U_∞ should be concentrated on the set where $\nabla K * U_\infty(y) - \beta y$ vanishes. In the community of granular flow, for a given U_∞, the corresponding self-similar solution $u(x,t) = t^\alpha U_\infty(xt^\beta)$ is called a homogeneous cooling state [12]; it is expected to play the same role as the Maxwellian distribution for the Boltzmann equation in rarefied gas dynamics.

However, because the energy $E(U)$ is not convex, the limit U_∞ above can be local minimizers or even saddle points. In general, the convergence of the solution

U to its limit U_∞ is so weak, there is no more information about U_∞ besides the characterizing equality (9).

2.2. **Convergence for radially symmetric solutions.** To get more quantitative properties about these limiting solutions U_∞, we consider only the radially symmetric ones $U_\infty(y) = U_\infty(r)$ with $r = |y|$ in the rest of this section. Denote the radial characteristic velocity, in similarity variables as

$$V(r) = \beta r - \frac{d}{dr} K * U_\infty. \tag{10}$$

Since U_∞ is a non-negative measure, $\frac{d^3}{dr^3}V(r) < 0$ on $(0,\infty)$ and $\frac{d^2}{dr^2}V(0) = 0$. Therefore $\frac{d^2}{dr^2}V(r)$ is concave and $V(r)$ has at most one zero r_0 on $(0,\infty)$, besides the obvious zero at the origin. In other words, from the equilibrium condition (9), $U_\infty(r)$ can only be supported at the origin and at r_0. If the fraction of mass concentrated at the origin is ν and the rest on the sphere of radius $r_{0,\nu}$ is $1-\nu$, then the limiting solution can be represented as

$$U_{\infty,\nu}(x) = \nu M \delta(x) + \frac{(1-\nu)M}{n\omega_n r_{0,\nu}^{n-1}} \delta(|x| - r_{0,\nu}), \tag{11}$$

where ω_n is the volume of the unit sphere in dimension n. Here the radius $r_{0,\nu}$ of the mass concentrating sphere can be solved from the equation $V(r_{0,\nu}) = 0$, i.e.,

$$r_{0,\nu} = \left(\frac{1}{\gamma M} \frac{\beta}{\nu + (1-\nu)2^{\gamma-1} B(\frac{n+\gamma-1}{2}, \frac{n-1}{2}) / B(\frac{n-1}{2}, \frac{n-1}{2})} \right)^{1/(\gamma-2)}, \tag{12}$$

where B is the Beta function. The corresponding energy is

$$E(U_{\infty,\nu}) = -\frac{(1-\nu)\beta M r_{0,\nu}^2}{2\gamma}. \tag{13}$$

We note that the limiting solutions $U_{\infty,\nu}$ for $\nu > 0$ are unstable. Since the corresponding radial characteristic velocity $V(r)$ is positive near the origin, any perturbation of mass from the origin will expand outward to the mass-concentrating sphere instead of moving inward. Therefore, the amount of mass νM concentrated at the origin is exactly that from the initial condition. Moreover, from the explicit expression (13), $U_{\infty,0}$ is the global minimizer of the energy (6) in the set of all radially symmetric measures while those $U_{\infty,\nu}$ with $\nu \neq 0$ are only saddle points of the energy. For generic radially symmetric initial data without any concentration of mass at the origin, the solution U converges to the global minimizer $U_{\infty,0}$ (denoted as U_∞ for simplicity). For this reason, we consider the asymptotic behavior of the solutions to U_∞ in the remaining sections and the generalization to the convergence to $U_{\infty,\nu}$, where $\nu > 0$ requires only minor modification.

2.3. **Asymptotic convergence to the δ-ring for radially symmetric solutions.** For smooth initial data $u_0(x)$ decaying fast enough, the solution $u(x,t)$ stays smooth but converges to a δ-ring with vanishing radius when t goes to infinity, while the corresponding solution $U(y,\tau)$ in similarity variables converges to a δ-ring with fixed radius, as shown in Figure 1 for $\gamma = 4$ in dimension three. The equations (1) and (4) are solved numerically by the method of characteristics. For example, the characteristic equations of the radial variables in (1) are

$$\frac{dr}{dt} = -\frac{\partial}{\partial r} K * u, \quad \frac{du}{dt} = u \Delta_r K * u, \tag{14}$$

where $\Delta_r = \frac{1}{r^{n-1}}\frac{\partial}{\partial r} r^{n-1}\frac{\partial}{\partial r}$ is the Laplacian. The detailed numerical scheme is discussed in the next section for the case $\gamma \in (0, 2)$, where we have to rely on numerics to guide the analysis because of the anomalous similarity solutions.

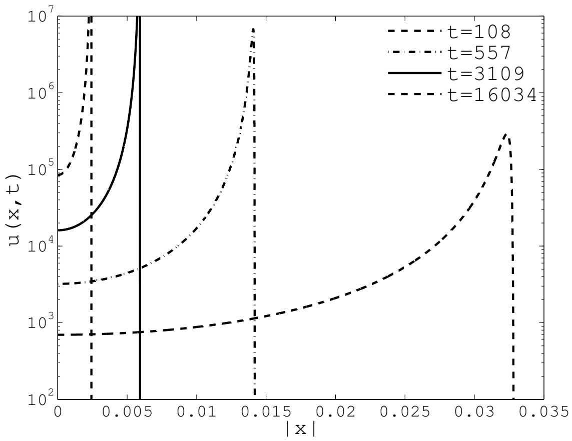

(**a**)

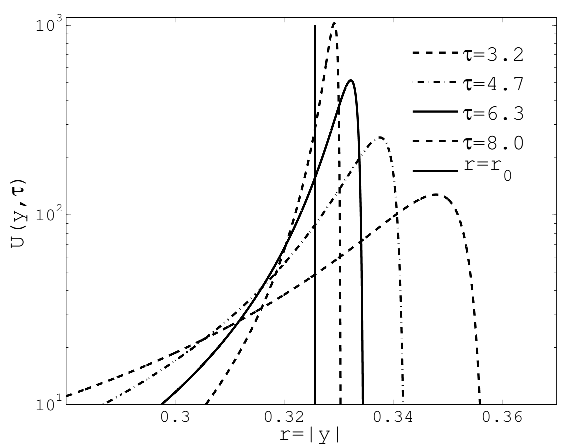

(**b**)

FIGURE 1. (**a**) Radially symmetric solution u for the original equation (1) and (**b**) the corresponding similiarity variable U for (4) at different time for $\gamma = 4$ in dimension three. The solution u converges to a δ-ring with vanishing radius while U converges to a δ-ring with radius $r_0 \approx 0.325$.

These figures reveal some non-trivial behavior of the convergence of the solution U towards the δ-ring. This brings the question of the large time, intermediate asymptotics of U. The key observation to derive the refined asymptotics is the fact that the first and second derivatives of the convolution $K * U$ converge to their limiting values much faster, as shown in Figure 2. In other words, for large τ, the characteristic speed $dr/d\tau$ and the rate of increase of the solution U along the characteristics become essentially steady. Therefore, the leading order large time asymptotics for U is governed by the linear first order equation

$$U_\tau = \nabla \cdot \left[U(\nabla K * U_\infty - \beta y)\right], \tag{15}$$

in which the convolution $K * U$ is replaced by the effective one $K * U_\infty$. With the radius r_0 of the limiting δ-ring computed from (12) with $\nu = 0$,

$$r_0 = \left(\frac{\beta}{2^{\gamma-1}\gamma M} \frac{B(\frac{n-1}{2}, \frac{n-1}{2})}{B(\frac{n+\gamma-1}{2}, \frac{n-1}{2})} \right)^{1/(\gamma-2)},$$

the system of ODEs for the characteristic variables r and U of (15) becomes

$$\frac{dr}{d\tau} = \beta r - \frac{M\gamma}{\int_0^\pi \sin^{n-2}\theta d\theta} \int_0^\pi (r - r_0\cos\theta)(r^2 + r_0^2 - 2rr_0\cos\theta)^{\gamma/2-1} \sin^{n-2}\theta d\theta,$$

$$\frac{dU}{d\tau} = \left(\frac{M\gamma(n+\gamma-2)}{\int_0^\pi \sin^{n-2}\theta d\theta} \int_0^\pi (r^2 + r_0^2 - 2rr_0\cos\theta)^{\gamma/2-1} \sin^{n-2}\theta d\theta - n\beta \right) U.$$

For $r < r_0$ near the origin, the above characteristic equations can be approximated as

$$\frac{dr}{d\tau} \approx A_0 r, \qquad \frac{dU}{d\tau} \approx (-B_0 + C_0 r^2)U, \tag{16}$$

where

$$A_0 = \beta\left(1 - \frac{\gamma-1}{2^{\gamma-2}} \frac{B(\frac{n-1}{2}, \frac{n-1}{2})}{B(\frac{n+\gamma-1}{2}, \frac{n-1}{2})}\right), \quad B_0 = \beta\left(n - \frac{n+\gamma-2}{2^{\gamma-2}} \frac{B(\frac{n-1}{2}, \frac{n-1}{2})}{B(\frac{n+\gamma-1}{2}, \frac{n-1}{2})}\right),$$

$$C_0 = M(n+\gamma-2)\gamma(\gamma-2)(\gamma-3)r_0^{\gamma-4}.$$

This local approximation leads to the asymptotic solution of the form

$$U(r,\tau) \sim e^{-B_0\tau + \frac{C_0}{2A_0}r^2}, \tag{17}$$

where the prefactor determined by the initial condition is transient and is therefore omitted. The time decay $U(0,\tau) \sim e^{-B_0\tau}$ at the origin and the spatial variation of $U(r,\tau) \sim U(0,\tau)e^{C_0 r^2/3}$ near the origin are confirmed numerically in Figure 3. Away from the origin the match in the spatial variation can be improved if higher order terms in r are included in (16).

For r close to r_0, the characteristic equations can be approximated as

$$\frac{dr}{d\tau} \approx -A_1(r - r_0), \qquad \frac{dU}{d\tau} \approx (B_1 - C_1(r - r_0))U, \tag{18}$$

where

$$A_1 = B_1 = (\gamma-2)\beta, \quad C_1 = \frac{(n+\gamma-2)\gamma(\gamma-2)\beta}{2r_0}.$$

This leads to the asymptotic solution of the form

$$U(r,\tau) \sim e^{B_1\tau - C_1 e^{A_1\tau}(r-r_0)/A_1}. \tag{19}$$

However, here the prefactor depends strongly on the decay rate of the initial condition, making it useful only at $r = r_0$; the increase rate $O(e^{B_1\tau})$ of U at this point is verified numerically in Figure 4.

In summary, for generic radially symmetric and smooth initial data, the approach of the solution U to the the limit U_∞ is therefore characterized by the asymptotic scaling (17) and (19). However, these asymptotic forms do not tell us anything about the convergence rate in probability metrics like the Wasserstein distances [1].

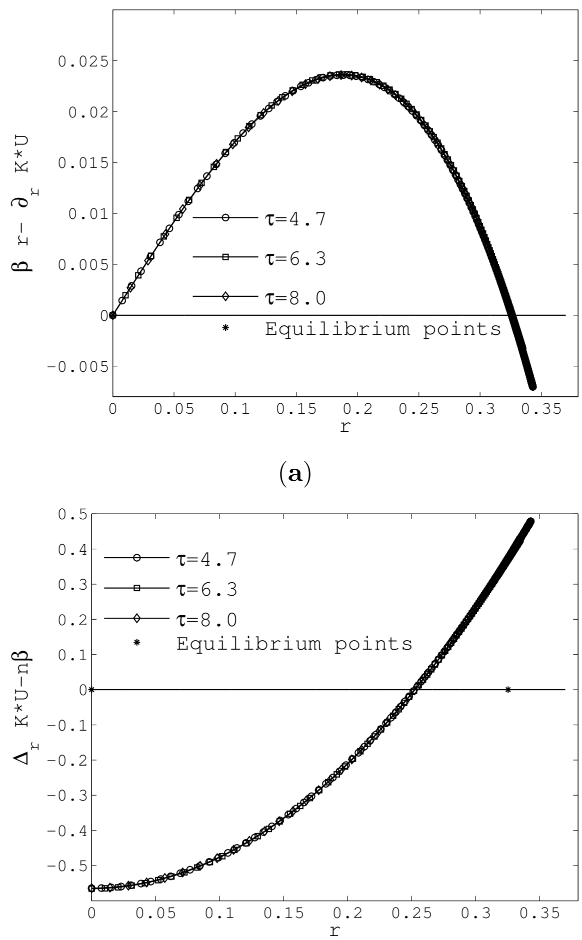

(**a**)

(**b**)

FIGURE 2. (**a**) The characteristic velocity $dr/d\tau$ and (**b**) the rate of change $\frac{1}{U}\frac{dU}{d\tau}$ for $\gamma = 4$ in dimension three. There are two equilibrium points for the characteristic velocity: the one at the origin is unstable; the one at $r_0 \approx 0.325$ is stable.

The convergence in these weaker spaces is in general much more difficult, even for solutions governed by the linearized equation (15).

3. **Finite time blowup for** $0 < \gamma < 2$**.** For $\gamma \in (0, 2)$, because of the relatively strong attraction between particles close enough, smooth solutions blow up in finite time [5]. If T is the blowup time, we can introduce the following similarity variables y and τ,

$$y = x(T-t)^{-\beta}, \quad \tau = -\ln(T-t) \tag{20}$$

and define $U(y, \tau)$ such that

$$u(x,t) = (T-t)^{-\alpha} U(x(T-t)^{-\beta}, \tau), \tag{21}$$

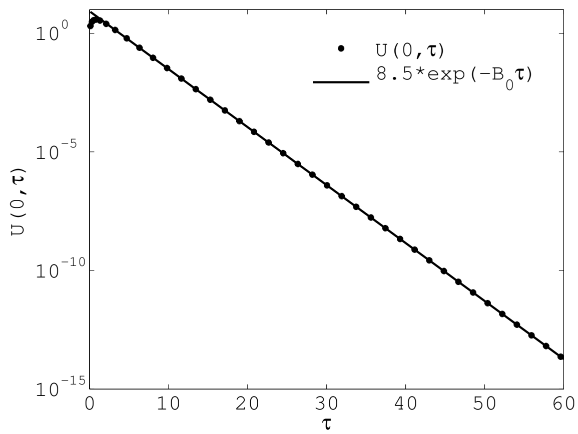

(**a**)

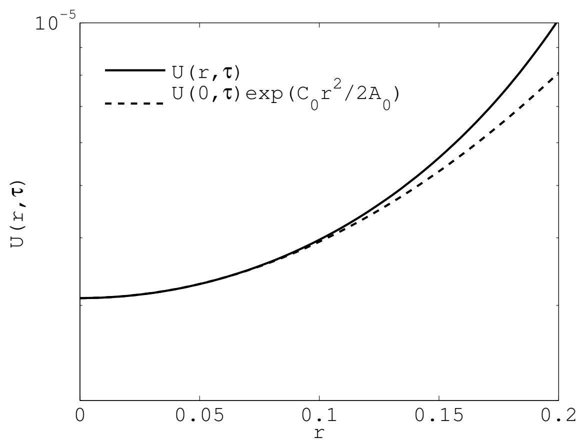

(**b**)

FIGURE 3. (**a**) The decay of U at the origin for $\gamma = 4$ in dimension three. (**b**) The spatial variation of U near the origin for the same dynamics at $\tau = 0.8$.

where α and β are unknown constants. Substituting (21) into (1), the resulting equation for U has no explicit dependence on τ only if

$$\alpha = (n + \gamma - 2)\beta + 1, \tag{22}$$

with the evolution equation

$$U_\tau = \nabla \cdot (U \nabla K * U) - \alpha U - \beta y \cdot \nabla U. \tag{23}$$

If finite mass is concentrated in the core of the blowup profile,

$$\alpha = n\beta \tag{24}$$

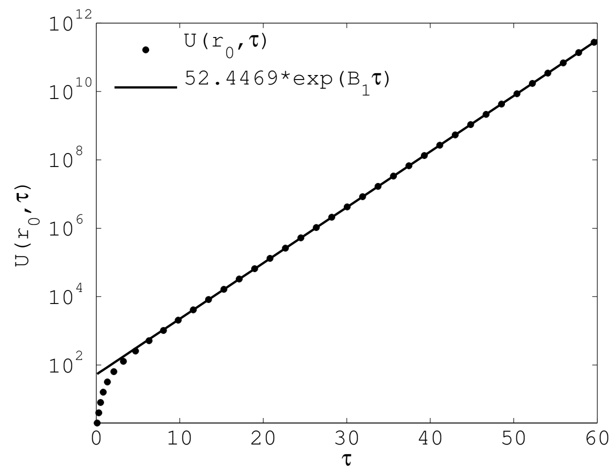

FIGURE 4. The increase of U at r_0 for $\gamma = 4$ in dimension three at $\tau = 8.0$.

must hold for the mass conservation of both u and U. This relation, together with (22), gives the exponents

$$\alpha = \frac{n}{2-\gamma}, \qquad \beta = \frac{1}{2-\gamma}, \tag{25}$$

characterizing self-similar solutions of the *first kind*. Any exact self-similar solutions of this form satisfy the steady state equation (23). However, it is shown in [5] that there are no such exact smooth self-similar solutions in odd dimensions for the special case $\gamma = 1$ and in [15] that the only radially symmetric ones are weak measures concentrated at the origin and at most one δ-ring. In fact, for generic radially symmetric, smooth initial data, the solution does not converge to the self-similar solutions of the first kind discussed above. In one dimension, the equation with the case $\gamma = 1$ can be transformed into Burgers equation. It is shown in [17] that $\beta = 1.5$ instead of $\beta = 1$ as from (25) and the corresponding self-similar solutions are of the second kind. It was also recently shown [6] that the multidimensional problem with Newtonian potential $K(x) = |x|^{2-n}$ can be transformed to Burgers equation in the case of radial symmetry. The change of variables gives $\beta = 3/2n$, using the same exact solution of Burgers equation that describes a generic singularity. For more general power-law kernels $K(x) = |x|^\gamma$, we must solve the problem numerically, and this is done in general dimensions for $\gamma = 1$ by the authors in [21]. The numerics shows a clear second kind similarity solution. The main point of this section is to show that this behavior holds for all $\gamma \in (0, 2)$.

3.1. **Numerical method and numerical results.** The numerical method is a slight generalization of that in [21] and is reviewed next for completeness. The equation (1) is solved by the method of characteristics, respecting the underlying transport structure of the dynamics. In radial coordinates, the original equation (1) can be written as

$$u_t = \frac{\partial u}{\partial r}\frac{\partial}{\partial r}K * u + u\Delta_r K * u, \tag{26}$$

where $\Delta_r = \partial_{rr} + \frac{n-1}{r}\partial_r$ is the Laplacian in the radial variable r. Therefore, the system of ODEs for the characteristics is

$$\frac{dr}{dt} = -\frac{\partial}{\partial r} K * u, \quad \frac{du}{dt} = u\Delta_r K * u. \tag{27}$$

More precisely,

$$\frac{\partial}{\partial r} K * u = \gamma c_n \int_0^\infty u(r')r'^{n-1} \int_0^\pi (r - r'\cos\theta) I(r,r')^{q-2} \sin^{n-2}\theta d\theta dr',$$
$$\Delta_r K * u = (n+\gamma-2)\gamma c_n \int_0^\infty u(r')r'^{n-1} \int_0^\pi I(r,r')^{q-2} \sin^{n-2}\theta d\theta dr',$$

where

$$I(r,r') = (r^2 + r'^2 - 2rr'\cos\theta)^{1/2}$$

and $c_n = (n-1)\omega_{n-1}$.

The integral in the angular variable θ can be precomputed as a function of r, r' and the ratio r'/r as a consequence of the homogeneity of the kernel. More precisely, we precompute the following integrals

$$\int_0^\pi (r - r'\cos\theta) I(r,r')^{q-2} \sin^{n-2}\theta d\theta$$
$$= \begin{cases} r^{\gamma-1} \int_0^\pi (1-\rho\cos\theta)(1+\rho^2-2\rho\cos\theta)^{\gamma/2-1} \sin^{n-2}\theta d\theta, & \text{if } \rho = r'/r \le 1, \\ (r')^{\gamma-1} \int_0^\pi (\rho-\cos\theta)(1+\rho^2-2\rho\cos\theta)^{\gamma/2-1} \sin^{n-2}\theta d\theta, & \text{if } \rho = r/r' \le 1, \end{cases}$$

and

$$\int_0^\pi I(r,r')^{q-2} \sin^{n-2}\theta d\theta = \max(r,r')^{\gamma-2} \int_0^\pi (1+\rho^2-2\rho\cos\theta)^{\gamma/2-1} \sin^{n-2}\theta d\theta,$$

where $\rho = \min(r,r')/\max(r,r') \in [0,1]$. With the auxiliary functions

$$I_1(\rho) = \int_0^\pi (1-\rho\cos\theta)(1+\rho^2-2\rho\cos\theta)^{\gamma/2-1} \sin^{n-2}\theta d\theta,$$
$$I_2(\rho) = \int_0^\pi (\rho-\cos\theta)(1+\rho^2-2\rho\cos\theta)^{\gamma/2-1} \sin^{n-2}\theta d\theta,$$
$$I_3(\rho) = \int_0^\pi (1+\rho^2-2\rho\cos\theta)^{\gamma/2-1} \sin^{n-2}\theta d\theta,$$

the complexity is reduced to $O(N^2)$ per time step to evaluate the integrals in the characteristic ODEs (27) using trapezoidal rule, where N is the number of spatial grid points in the radial coordinate r. Once the characteristic speeds in (27) are found, the system (26) is evolved using the classical fourth-order Runge-Kutta method. The anomalous exponent β and the self-similar profile U can be obtained by post-processing of the solution or using numerical renormalization method as in [21].

We have shown sample results in the previous section for $\gamma > 2$ and focus on the exponents β and the profiles for $\gamma \in (0,2)$ in the rest for second kind similarity solutions. The blowup profiles for $\gamma = 1$ in different dimensions and for different γ in dimension three are shown in Figure 5-6, respectively. The profiles are ordered in the far field but not near the origin, and are qualitatively the same for other fixed γ or fixed dimensions. The anomalous exponents for different γ in different dimensions are shown in Figure 7. These exponents have a strong dependence on the power γ but a very weak dependence on the dimension n. Though there is no explicit formula for these exponents, the asymptotic behavior of β is evident when γ is close to zero or two, both of which are analyzed next after some properties of these self-similar profiles are reviewed.

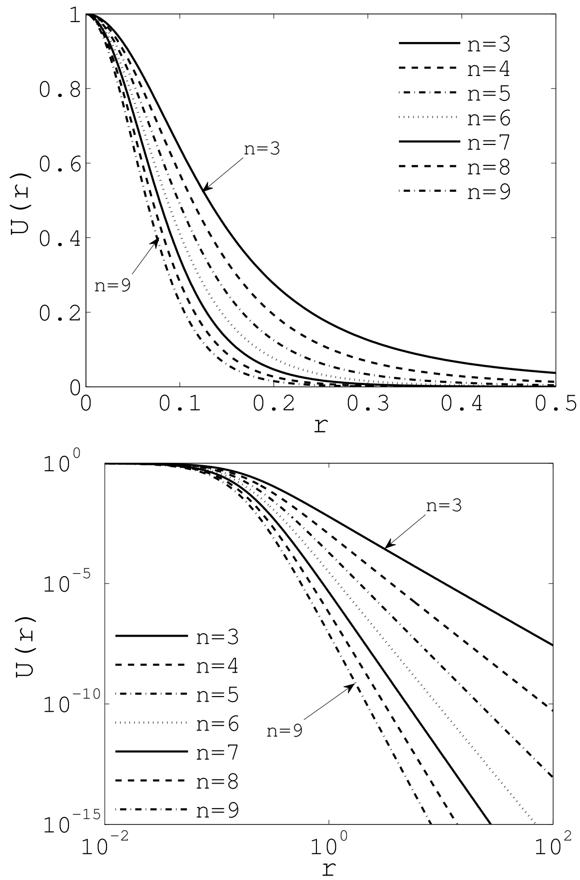

FIGURE 5. Blowup profiles in the similarity variables U and r, in different space dimensions for $\gamma = 1$.

3.2. **Properties of the self-similar profile U.** The self-similar profile U, if it exists, must satisfy the steady state of (23),

$$\mathcal{A}U \equiv \nabla \cdot (U \nabla K * U) - \alpha U - \beta y \cdot \nabla U = 0. \tag{28}$$

A few properties of U are immediately available. First there is actually a family of solutions: if U is a solution of (28), so is $U_\lambda(y) = \lambda^{n+\gamma-2} U(\lambda y)$ for any $\lambda > 0$. As a result, all the profiles U shown in Figure 5-6 and analyzed below are normalized by the condition $U(0) = 1$. Moreover, this family of solutions gives arise to an eigenpair for the linearized operator $\mathcal{L}$ at U defined as

$$\mathcal{L}W \equiv \nabla \cdot (U \nabla K * W) + \nabla \cdot (W \nabla K * U) - \alpha W - \beta y \cdot \nabla W. \tag{29}$$

In fact, from the invariance of the solution U_λ,

$$0 = \frac{d}{d\lambda} \mathcal{A} U_\lambda \bigg|_{\lambda=1} = \mathcal{L}\, \frac{d}{d\lambda} U_\lambda \bigg|_{\lambda=1} = \mathcal{L}\left[(n+\gamma-2)U + y \cdot \nabla U\right]. \tag{30}$$

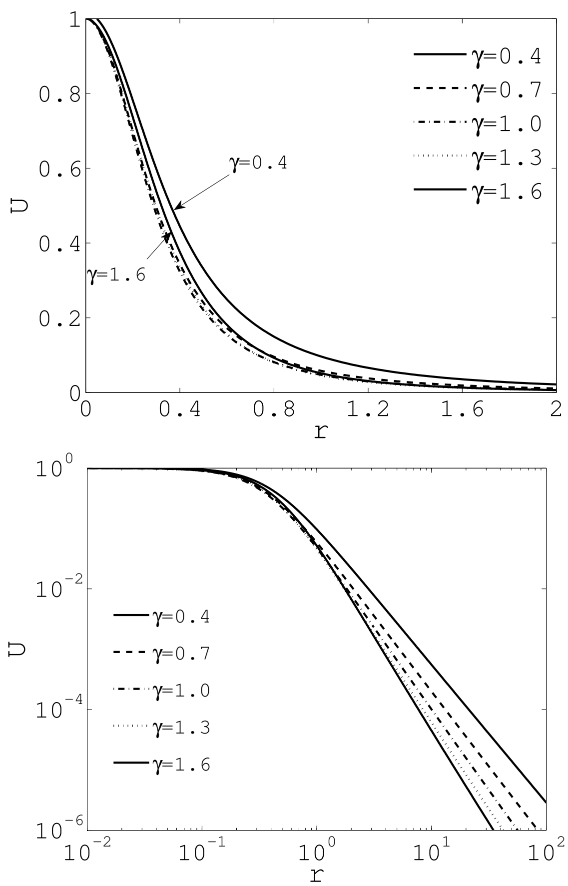

FIGURE 6. Blowup profiles in the similarity variables U and r, in dimension three for different γ.

This implies that $e_1(y) = (n+\gamma-2)U + y\cdot\nabla U$ is an eigenfunction of $\mathcal{L}$ corresponding to the eigenvalue zero. From this eigenpair and the steady state equation (28), we can get the second eigenpair:

$$\mathcal{L}\left[\alpha U + \beta y\cdot\nabla U\right] = \mathcal{L}(U) = \alpha U + \beta y \cdot \nabla U, \tag{31}$$

or $e_2(y) = \alpha U + \beta y\cdot\nabla U$ is the eigenfunction of $\mathcal{L}$ corresponding to eigenvalue one. This second eigenpair is related to the time translation of the solution $u(x,t) = (T-t)^{-\alpha}U(x(T-t)^{-\beta})$. More precisely, if the time t is translated to $t+\epsilon$ or

$$T - t - \epsilon = (T-t)(1-\epsilon e^{\tau}),$$

then

$$\begin{aligned} u^{\epsilon}(x,t) &= (T-t-\epsilon)^{-\alpha}U(x(T-t-\epsilon)^{-\beta}) \\ &= (T-t)^{-\alpha}(1-\epsilon e^{\tau})^{-\alpha}U(x(T-t)^{-\beta}(1-\epsilon e^{\tau})^{-\beta}) \\ &= u(x,t) + \epsilon(T-t)^{-\alpha-1}e_2(x(T-t)^{-\beta}) + O(\epsilon^2). \end{aligned}$$

Even though this eigenvalue is positive, the blowup profile is stable; any perturbation in this mode results only in a translation in the blowup time. However, this

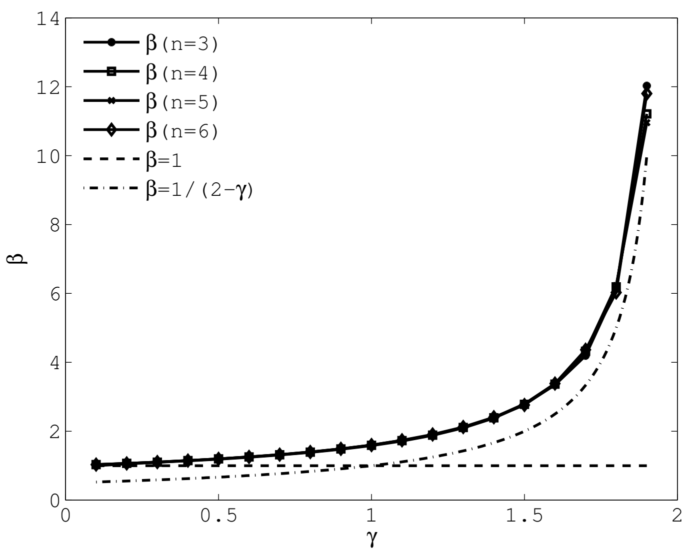

Figure 7. The anomalous exponents β in different dimensions for $\gamma \in (0, 2)$. The exponents have a very weak dependence on the dimension, but a strong dependence on γ.

mode does prevent any direct computation of the profile U from (23), unless the dynamics is restricted to the space orthogonal to e_2.

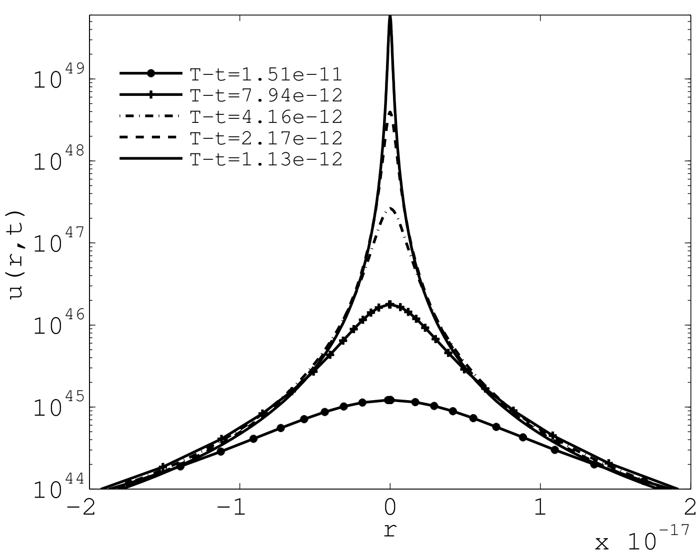

Figure 8. The solution near the blowup time for $\gamma = 1$ in dimension three, which collapses into the envelope $|x|^{-\alpha/\beta}$.

Another important property is the algebraic decay rate of U in the far field. All the solutions u are observed to collapse into one envelope (Figure 8). This, together with the ansatz (21), implies that $U(y) \sim |y|^{-\alpha/\beta} = |y|^{2-n-\gamma-1/\beta}$ as $|y|$ goes to infinity. This decay rate provides another validation for the numerical results and an extra self-consistent condition for the perturbation expansion below as γ goes to 2^-.

3.3. **The asymptotics when $\epsilon = \gamma \to 0$.** In general, the exponent β in the second-kind self-similar solution is governed by a nonlinear eigenvalue problem [2] and there is no explicit formula as in the first-kind counterpart. However, for the special case of $K(x) = |x|$ in odd dimension, the exponents are calculated in [22, 20] by transforming the steady state equation (28) into a system of ODEs, followed a shooting method to match the boundary conditions of these two. Furthermore, it is evident from Figure 7 that the exponent β has an asymptotic limit when γ approaches 0^+ and 2^-, which is the subject of this and the next subsection.

When $\epsilon = \gamma$ is close to 0, we first rescale the solution $U_\epsilon(y)$ to $W_\epsilon(y) = U_\epsilon(\epsilon^{1/(n+\epsilon-2)}y)$, since it is W_ϵ instead of U_ϵ that has a well-defined limit. This rescaling keeps the exponents α_ϵ and β_ϵ invariant, since the governing equation for W_ϵ is the same as for U_ϵ except with the rescaled kernel $\tilde{K}_\epsilon(x) = |x|^\epsilon/\epsilon$, i.e.,

$$\nabla \cdot (W_\epsilon \nabla \tilde{K}_\epsilon * W_\epsilon) = \alpha_\epsilon W_\epsilon + \beta_\epsilon y \cdot \nabla W_\epsilon. \tag{32}$$

The numerically computed β in Figure 7 suggests the following asymptotic expansions for the exponents

$$\beta_\epsilon = 1 + C_1\epsilon + C_2\epsilon^2 + \cdots, \tag{33a}$$

$$\alpha_\epsilon = (n-2+\epsilon)\beta_\epsilon + 1 = n - 1 + ((n-2)C_1 + 1)\epsilon + \cdots, \tag{33b}$$

and for the profile

$$W_\epsilon = W_0 + \epsilon W_1 + \epsilon^2 W_2 + \cdots. \tag{34}$$

Upon substituting them into (32), the resulting leading order $O(1)$ equation is

$$\nabla \cdot (W_0 \nabla \tilde{K}_0 * W_0) = (n-1)W_0 + y \cdot \nabla W_0, \qquad \tilde{K}_0(x) = \ln |x| \tag{35}$$

with the boundary conditions

$$W_0(0) = 1, \quad \nabla W_0(y)|_{y=0} = 0, \quad W_0(y) \sim |y|^{1-n} \quad \text{as } |y| \to \infty. \tag{36}$$

Compared with the steady equation (28) for general γ (or ϵ), the integral-differential equation (35) for the limiting profile contains no unknown parameters. To get the first order correction for β, we introduce the linearized operator $\mathcal{L}_0$ at W_0

$$\mathcal{L}_0(V) \equiv \nabla \cdot (V \nabla \tilde{K}_0 * W_0) + \nabla \cdot (W_0 \nabla \tilde{K}_0 * V) - (n-1)V - y \cdot \nabla V, \tag{37}$$

and its formal adjoint operator

$$\mathcal{L}_0^*(V) \equiv -\nabla V \cdot \nabla \tilde{K}_0 * W_0 + \nabla \cdot \int_{\mathbb{R}^n} \tilde{K}_0(y-z) W_0(z) \nabla V(z) dz + V + y \cdot \nabla V.$$

It is obvious that we obtain from the steady state equation (35) that

$$\mathcal{L}_0(W_0) = (n-1)W_0 + y \cdot \nabla W_0 \tag{38}$$

and from the explicit eigenpair (30) that

$$\mathcal{L}_0 \left[(n-2)W_0 + y \cdot \nabla W_0\right] = 0. \tag{39}$$

The $O(\epsilon)$ equation from (32) is

$$\mathcal{L}_0(W_1) = ((n-2)C_1+1)W_0 + C_1 y\cdot\nabla W_0 - \nabla\cdot\left[W_0\left(\frac{y}{|y|^2}\ln|y|\right)*W_0\right]$$
$$= C_1\mathcal{L}_0(W_0) - C_1W_0 - \nabla\cdot\left[W_0\left(\frac{y}{|y|^2}\ln|y|\right)*W_0\right]. \tag{40}$$

We can now find C_1 from the solvability condition. Since $\mathcal{L}_0$ has a one-dimensional null space, spanned by $(n-2)W_0 + y\cdot\nabla W_0$, the formal adjoint $\mathcal{L}_0^*$ is expected to have a non-trivial null space too, containing a nonzero function W_0^* such that $\mathcal{L}_0^*(W_0^*) = 0$. The solvability condition for (40) is then obtained by multiplying both sides with W_0^* and integrating on the whole space, i.e.

$$0 = \int_{\mathbb{R}^n} W_0^*\left(C_1\mathcal{L}(W_0) - C_1W_0 - \nabla\cdot\left[W_0\left(\frac{y}{|y|^2}\ln|y|\right)*W_0\right]\right)dy$$
$$= -C_1\int_{\mathbb{R}^n} W_0^*W_0dy - \int_{\mathbb{R}^n} W_0^*\nabla\cdot\left[W_0\left(\frac{y}{|y|^2}\ln|y|\right)*W_0\right]dy. \tag{41}$$

This gives the coefficient C_1 for the first order correction of β_ϵ as

$$C_1 = -\frac{1}{\int_{\mathbb{R}^n} W_0^*W_0dy}\int_{\mathbb{R}^n} W_0^*\nabla\cdot\left[W_0\left(\frac{y}{y|^2}\ln|y|\right)*W_0\right]dy. \tag{42}$$

Since both the leading order profile equation (35) and the adjoint equation $\mathcal{L}_0^*(W^*) = 0$ are nonlinear nonlocal, there is no explicit form for the exact solutions and they are also very challenging to solve numerically. In the special case of even dimensions, we can use the fact that successive Laplacians of the kernel $\tilde{K}_0(y) = \ln|y|$ becomes the fundamental solution of the Laplace equation. This allows us to compute the convolution $\tilde{K}_0 * W_0$ by a system of ODEs. This observation enables us to transform both integro-differential equations into two systems of ODEs by shooting methods, in the same spirit as calculating the exponent β for the special case $\gamma = 1$ in [20, 22].

We start with dimension $n = 4$, and the case in higher even dimensions can be generalized similarly. We introduce the scalar variables $w_0(r)(= W_0(|y|))$, $w_1(r)$, $w_2(r)$ and $w_3(r)$ defined on $[0,\infty)$, such that

$$w_3 = \frac{d}{dr}\tilde{K}_0 * w_0, \quad w_2 = \Delta_r\tilde{K}_0 * w_0, \quad w_1 = w_2', \tag{43}$$

where, by abuse of notion, the convolution is always performed on $\mathbb{R}^n$, but evaluated at $r = |y|$. Upon this change of variables, the governing equation (35) becomes

$$16\pi^2\left(\frac{dw_0}{dr}w_3 + w_0w_0\right) = 3w_0 + r\frac{dw_0}{dr}. \tag{44}$$

Therefore, the above system of ODEs can be rewritten as

$$\frac{dw_0}{dr} = -\frac{16\pi^2w_2 - 3}{16\pi^2w_3 - r}w_0, \tag{45a}$$
$$\frac{dw_1}{dr} = -w_0 - \frac{3}{r}w_1, \tag{45b}$$
$$\frac{dw_2}{dr} = w_1, \tag{45c}$$
$$\frac{dw_3}{dr} = w_2 - \frac{3}{r}w_3. \tag{45d}$$

This system is equivalent to (35) in the sense that $W_0(y) = w_0(r)$ with $r = |y|$, provided that the initial conditions at $r = 0$ and far field conditions as r goes to infinity match each other. The expected decay rate $O(r^{1-n})$ for w_0 implies that both w_1 and w_2 converge to zero as r goes to infinity and the shooting method is used to choose $w_i(0)$s appropriately to enforce these decay conditions in the far field. The dimension $n = 4$ is special because these initial conditions are determined completely by the local well-posedness of the system (45), i.e,

$$w_1(0) = 0, \quad w_2(0) = 3/16\pi^2, \quad w_3(0) = 0, \tag{46}$$

and $w_0(0) = 1$ for normalization. To avoid the singularity at the origin, the system (45) is calculated with any ODE solver starting at small $r > 0$, where the solution can be represented as a rapidly converging power series [20, 22].

Once the profile $w_0(= W_0)$ is found, the solution (or the eigenfunction) to the adjoint equation $\mathcal{L}_0^*(W_0^*) = 0$ is obtained similarly. Let $w_0^* = W_0^*$ and $\frac{d}{dr}w_1^* = W_0\frac{y}{|y|}\cdot\nabla W_0^*$, then the second term in $\mathcal{L}_0^*(W_0^*)$ can be rewritten as

$$\nabla\cdot\int_{\mathbb{R}^n}\nabla w_1^*(y)\ln|x-y|dy = -\nabla\cdot\int_{\mathbb{R}^n} w_1^*(y)\nabla_y\ln|x-y|dy = \Delta_r\ln|x| * w_1^*.$$

Denote the last convolution integral $\Delta_r\ln|x| * w_1^*$ as w_3^* and let $w_2^* = \frac{d}{dr}w_3^*$. Then the system of ODEs for the variables associated with the adjoint equation $\mathcal{L}_0^*(W_0^*) = 0$ becomes

$$\frac{dw_0^*}{dr} = -\frac{16\pi^2 w_2^* + w_0^*}{16\pi^2 w_3^* - r}, \tag{47a}$$

$$\frac{dw_1^*}{dr} = -\frac{16\pi^2 w_2^* + w_0^*}{16\pi^2 w_3^* - r}w_0, \tag{47b}$$

$$\frac{dw_2^*}{dr} = -w_1^* - \frac{3}{r}w_2^*, \tag{47c}$$

$$\frac{dw_3^*}{dr} = w_2^*. \tag{47d}$$

The initial condition $w_0^*(0) = 1$ is chosen for normalization in the one-dimensional family of solutions. By the local well-posedness of the above system and the even symmetry of w_1^* and w_3^*, we must have $w_2^*(0) = -w_0^*(0) = -1/16\pi^2$ and $w_2^*(0) = 0$. This leaves the problem of finding the shooting parameter $w_3^*(0)$ such that $w_0(r)$ goes to zero as r goes to infinity. Once both the profile w_0 and the solution w_0^* to the adjoint equation are found, the coefficient in the first order correction of β can be evaluated from (42). The comparison of this correction with the numerically computed β is shown in Figure 9, where C_1 estimated from (42) is approximately 2.17 in dimension four. In higher dimensions, the two systems of ODEs (45) and (47) can be solved similarly, with more shooting parameters (or initial conditions) and are therefore more difficult to solve [22].

3.4. **The asymptotics when $\epsilon = 2 - \gamma \to 0$.** When $\gamma \to 2^-$, the asymptotic expansions suggested from Figure 7 are

$$\beta_\epsilon = \frac{C_0}{\epsilon} + C_1 + C_2\epsilon + \cdots, \tag{48a}$$

$$\alpha_\epsilon = (2-\epsilon)\beta_\epsilon + 1 = \frac{nC_0}{\epsilon} + (nC_1 - C_0 + 1) + \cdots. \tag{48b}$$

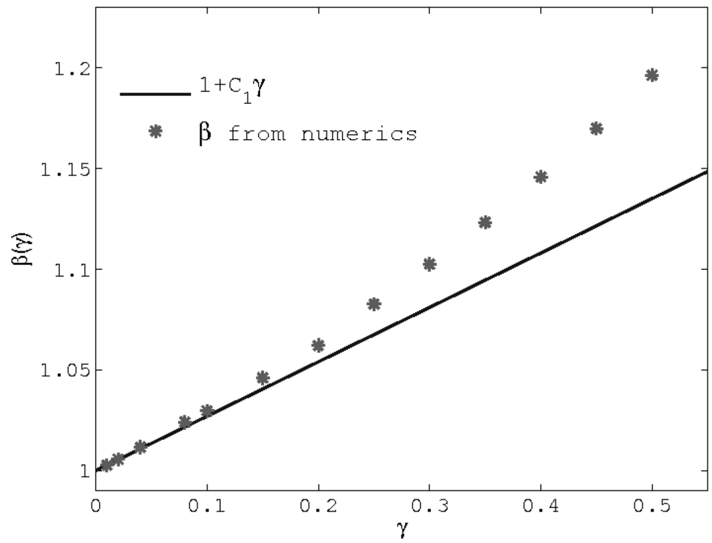

FIGURE 9. The comparison of the first order correction and the numerically computed β in dimension four. Here C_1 estimated from (42) is approximately 2.17.

Unlike the previous case when $\gamma \to 0^-$, because of the relatively slow decay of the integrand in the convolution, two asymptotic expansions

$$U_\epsilon = U_0 + \epsilon U_1 + \epsilon^2 U_2 + \cdots \tag{49a}$$

and

$$U_\epsilon = \tilde{U}_\epsilon(1 + \epsilon W_1 + \epsilon^2 W_2 + \cdots) \tag{49b}$$

are employed, where

$$\begin{aligned}\tilde{U}_\epsilon &= [U_0]^{1+\epsilon v_1 + \epsilon^2 v_2 + \cdots} \\ &= U_0 \left[1 + \epsilon v_1 \ln U_0 + \epsilon^2 \left(v_2 \ln U_0 + \frac{1}{2} v_1^2 \ln^2 U_0\right) + \cdots \right]\end{aligned} \tag{50}$$

for some constants v_1,v_2,$\cdots$. The first one (49a) is uniform when $|y|$ is close to the origin while the second one (49b) is uniform when $|y|$ is large and is the one that has to be used in the convolution. Here $\tilde{U}_\epsilon$ characterizes the power-law decay of the solution U_ϵ and W_is change slower than any power at infinity. These two asymptotic expansions are related, for example

$$U_1 = U_0(W_1 + v_1 \ln U_0).$$

The non-uniformity of the first one (49a) is obvious, because of the factor $\ln U_0$ in U_1 for any $v_1 \neq 0$.

The constants v_1, v_2, $\cdots$, can be calculated from the relation between the expected leading order decay of $U_0(y) \sim |y|^{-n}$ and that of $U_\epsilon(x) \sim |y|^{-\alpha_\epsilon/\beta_\epsilon}$, i.e.,

$$n(1 + \epsilon v_1 + \epsilon^2 v_2 + \cdots) = \frac{\alpha_\epsilon}{\beta_\epsilon} = n - \epsilon + \frac{1}{\beta_\epsilon}. \tag{51}$$

This gives

$$v_1 = \frac{1}{n}\left(\frac{1}{C_0} - 1\right), \quad v_2 = -\frac{C_1}{nC_0^2}, \quad \cdots . \tag{52}$$

For bounded y, using (49a), the right hand side of the steady state

$$\nabla \cdot (U_\epsilon \nabla K^\epsilon * U_\epsilon) = \alpha_\epsilon U_\epsilon + \beta_\epsilon y \cdot \nabla U_\epsilon, \qquad K^\epsilon(y) = |y|^{2-\epsilon} \tag{53}$$

becomes

$$\frac{C_0}{\epsilon}\nabla \cdot (yU_0(y)) + [C_1 \nabla \cdot (yU_0(y)) + C_0 \nabla \cdot (yU_1(y)) + (1 - C_0)U_0(y))]$$
$$+ \epsilon[C_2 \nabla \cdot (yU_0(y)) + C_1 \nabla \cdot (yU_1(y)) + C_0 \nabla \cdot (yU_2(y)) + (1 - C_0)U_1 - C_1 U_0] + \cdots$$

The left hand of the steady state (53) can be written as

$$\begin{aligned} &U_\epsilon(y) \int_{\mathbb{R}^n} \Delta K^\epsilon(y - y')U_\epsilon(y')dy' + \nabla U_\epsilon(y) \cdot \int_{\mathbb{R}^n} \nabla K^\epsilon(y - y')U_\epsilon(y')dy' \\ &= (2n - (n + 2)\epsilon + \epsilon^2)U_\epsilon(y) \int_{\mathbb{R}^n} |y - y'|^{-\epsilon} U_\epsilon(y')dy' \\ &\quad + (2 - \epsilon)\nabla U_\epsilon(y) \cdot \int_{\mathbb{R}^n} (y - y')|y - y'|^{-\epsilon} U_\epsilon(y')dy' \end{aligned} \tag{54}$$

We are going to use the expansion (49a) for $U_\epsilon(y)$ and (49b) for $U_\epsilon(y')$ in the above expression, where the $O(\epsilon^{-1})$ constant term arises from the convolution integrals for the slow algebraic decay of the integrand. When $|y'|$ is large, $|y - y'|^{-\epsilon}$ can be expanded as

$$\begin{aligned} |y - y'|^{-\epsilon} &= |y'|^{-\epsilon} \exp\left(-\epsilon \ln \frac{|y - y'|}{|y'|}\right) \\ &= |y'|^{-\epsilon}\left[1 - \epsilon \ln \frac{|y - y'|}{|y'|} + \frac{\epsilon^2}{2} \ln^2 \frac{|y - y'|}{|y'|} + \cdots\right]. \end{aligned}$$

The non-uniformity when $|y - y'|$ is small turns out to be unimportant since the associated integrals are absolutely integrable.

To further facilitate the calculation, we assume the following asymptotic form of the integrals

$$\int_{\mathbb{R}^n} |y'|^{-\epsilon} \tilde{U}_\epsilon(y')dy' = \frac{A_0}{\epsilon} + A_1 + \epsilon A_2 + \cdots , \tag{55a}$$

$$\int_{\mathbb{R}^n} |y'|^{-\epsilon} \tilde{U}_\epsilon(y')W_1(y')dy' = \frac{B_0}{\epsilon} + B_1 + \epsilon B_2 + \cdots , \tag{55b}$$

$$\int_{\mathbb{R}^n} |y'|^{-\epsilon} \tilde{U}_\epsilon(y')W_2(y')dy' = \frac{D_0}{\epsilon} + D_1 + \epsilon D_2 + \cdots . \tag{55c}$$

The exact values of these constants A_i, B_i and D_i are not used in the derivation of the leading order equation, as shown later.

With all the expansions above, keeping all terms up to $O(\epsilon)$, the first term in (54) can be simplified as

$$\begin{aligned} & (2n - (n + 2)\epsilon + \epsilon^2)\,[U_0(y) + \epsilon U_1(y) + \cdots] \\ & \int_{\mathbb{R}^n} |y - y'|^{-\epsilon} \tilde{U}_\epsilon(y')(1 + \epsilon W_1(y') + \cdots)dy' \\ = \quad & 2nU_0(y) \int_{\mathbb{R}^n} |y'|^{-\epsilon}\left(1 + \epsilon W_1(y') + \epsilon^2 W_2(y')\right)\tilde{U}_\epsilon(y')dy' \end{aligned}$$

$$
\begin{aligned}
&+\epsilon(2nU_1(y)-(n+2)U_0(y))\int_{\mathbb{R}^n}(1+\epsilon W_1(y'))\tilde{U}_\epsilon(y')dy' \\
&+\epsilon(2nU_2(y)-(n+2)U_1(y)+U_0(y))\int_{\mathbb{R}^n}|y'|^{-\epsilon}\tilde{U}_\epsilon(y')dy' \\
&-2\epsilon nU_0(y)\int_{\mathbb{R}^n}|y'|^{-\epsilon}\tilde{U}_\epsilon(y')\ln\frac{|y-y'|}{|y'|}dy'+O(\epsilon^2) \\
=\;& 2nU_0(y)(\frac{A_0}{\epsilon}+(A_1+B_0)+\epsilon(A_2+B_1+D_0)) \\
&+(2nU_1(y)-(n+2)U_0(y))(A_0+\epsilon(A_1+B_0)) \\
&+\epsilon(2nU_2(y)-(n+2)U_1(y)+U_0(y))A_0 \\
&-2\epsilon nU_0(y)\int_{\mathbb{R}^n}U_0(y')\ln\frac{|y-y'|}{|y'|}dy'+O(\epsilon^2),
\end{aligned}
$$

and the second term in (54) as

$$
\begin{aligned}
&(2-\epsilon)\left[\nabla U_0(y)+\epsilon\nabla U_1(y)+\cdots\right] \\
&\int_{\mathbb{R}^n}(y-y')|y-y'|^{-\epsilon}\tilde{U}_\epsilon(y')(1+\epsilon W_1(y')+\cdots)dy' \\
=\;& 2y\cdot\nabla U_0(y)(\frac{A_0}{\epsilon}+(A_1+B_0-\frac{A_0}{n})+\epsilon(A_2+B_1+D_0-\frac{A_1}{n}-\frac{B_0}{n})) \\
&+x\cdot\nabla(2U_1(y)-U_0(y))(A_0+\epsilon(A_1+B_0+\frac{A_0}{n})) \\
&-2\epsilon y\cdot\nabla U_0(y)\int_{\mathbb{R}^n}U_0(y')\ln\frac{|y-y'|}{|y'|}dy' \\
&+2\epsilon\nabla U_0(y)\cdot\int_{\mathbb{R}^n}y'U_0(y')\left(\ln\frac{|y-y'|}{|y'|}+\frac{y\cdot y'}{|y'|^2}\right)dy'+O(\epsilon^2).
\end{aligned}
\tag{56}
$$

Therefore, the leading order $O(\frac{1}{\epsilon})$ equation of (53) is

$$
2A_0\nabla\cdot(yU_0(y))=C_0\nabla\cdot(yU_0(y)) \tag{57}
$$

which gives $C_0=2A_0$.

The $O(1)$ equation is

$$
(C_0-1)U_0(y)+\left(2A_1+2B_0-\frac{n+2}{n}A_0-C_1\right)\nabla\cdot(yU_0(y))=0. \tag{58}
$$

There exists a non-trivial solution $U_0(y)$ satisfying the boundary condition $U_0(0)=1$ and $U_0(y)\sim|y|^{-n}$ only when both coefficients vanish, i.e.,

$$
C_0=1,\quad 2A_1+2B_0-C_1=\frac{n+2}{2n}. \tag{59}
$$

Finally the order $O(\epsilon)$ equation is

$$
\begin{aligned}
&C_1U_0(y)+\left(2A_2+2B_1+2D_0-\frac{n+2}{n}(A_1+B_0)-C_1\right)\nabla\cdot(yU_0(y)) \\
&=2\nabla\cdot(yU_0(y))\int_{\mathbb{R}^n}U_0(y')\ln\frac{|y-y'|}{|y'|}dy' \\
&-2\nabla U_0(y)\cdot\int_{\mathbb{R}^n}y'U_0(y')\left(\ln\frac{|y-y'|}{|y'|}+\frac{(y,y')}{|y'|^2}\right)dy'.
\end{aligned}
\tag{60}
$$

Evaluating the above equation at $y = 0$, we get

$$n\left(2A_2 + 2B_1 + 2D_0 - \frac{n+2}{n}(A_1 + B_0) - C_1\right) + C_1 = 0 \tag{61}$$

As a result, the governing equation (60) can be simplified as

$$\frac{C_1}{n} y \cdot \nabla U_0(y) = 2\nabla U_0(y) \cdot \int_{\mathbb{R}^n} y' U_0(y') \left(\ln \frac{|y - y'|}{|y'|} + \frac{y \cdot y'}{|y'|^2}\right) dy'$$
$$- 2\nabla \cdot (y U_0(y)) \int_{\mathbb{R}^n} U_0(y') \ln \frac{|y - y'|}{|y'|} dy'. \tag{62}$$

The unknown constant C_1 can be determined from the self-consistent condition of the above equation when $|y|$ goes to infinity. Since the $U_0(y)$ decays like $O(|y|^{-n})$, so does the left hand side of (62). This decay is balanced by the first term on the right hand side since $\nabla \cdot (y U_0(y)) \sim o(|y|^{-n})$. More precisely, the constant C_1 satisfies the condition

$$\frac{C_1}{n} y \cdot \nabla U_0(y) \approx 2\nabla U_0(y) \cdot \int_{\mathbb{R}^n} y' U_0(y') \left(\ln \frac{|y - y'|}{|y'|} + \frac{y \cdot y'}{|y'|^2}\right) dy' \tag{63}$$

as $|y| \to \infty$, or equivalently

$$C_1 = \lim_{|y|\to\infty} \frac{2}{|y|^2} \int_{\mathbb{R}^n} y \cdot y' U_0(y') \left(\ln \frac{|y - y'|}{|y'|} + \frac{y \cdot y'}{|y'|^2}\right) dy'. \tag{64}$$

In general, the coefficient C_1 can only be estimated from (64) using any numerically calculated profile U_0 when γ is close to 2. The comparison of the numerical computed β and its first order asymptotic expansion is shown in Figure 10, where $C_1(\approx 1.42)$ is estimated from (64) with the limiting profile U_0 calculated with $\gamma = 1.98$ and the limit taken at $|y| = 10^5$.

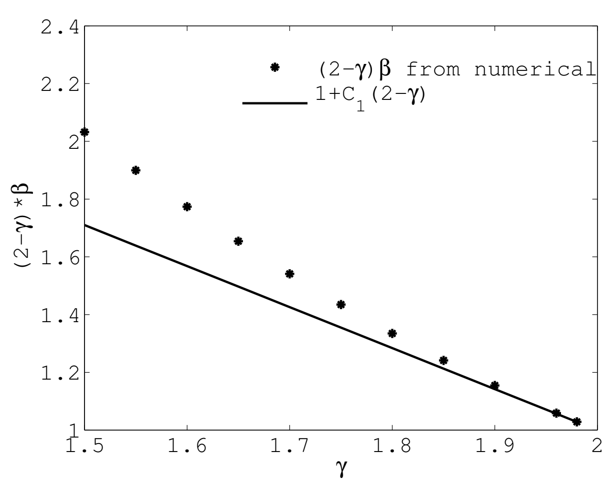

FIGURE 10. The comparison of the first order correction and the numerically computed β (rescaled by $2 - \gamma$) in dimension four. Here $C_1(\approx 1.42)$ is estimated from (64) with the limiting profile U_0 calculated with $\gamma = 1.98$ and the limit taken at $|y| = 10^5$.

4. **Conclusion.** We have analyzed the asymptotic behavior of two types of blowup solutions to the aggregation equation $u_t = \nabla \cdot (u \nabla K * u)$, depending on the power of the homogeneous kernel $K(x) = |x|^\gamma$. The phenomena when $\gamma > 2$ is studied thoroughly for the one-dimensional granular flow [32, 3], but the anomalous scaling in the self-similar solutions are studied only recently in [21]. This paper gives a complete picture of the generic radially symmetric blowup solutions for this simple kernel, whose analysis is guided heavily by numerical simulations, especially the asymptotic behavior of the anomalous exponent when γ is close to 0 and 2. These results are actually true for a larger class of non-smooth radially symmetric initial condition. For instance, as long as initially there is mass around the origin, the solution still exhibits second-kind self-similarity, reflecting the connection between this anomaly and the conservation of total mass. However, the stability of these solutions under non-radial perturbation and the possibility of other (stable or unstable) self-similar solutions remains unknown and is challenging numerically too. Another important generalization is the introduction of additional smoothing effects, like degenerate or fractional diffusion. This may lead to more physical steady state solutions instead of the singular ones considered here. We also note that the recent work [6] proves existence of blowup solutions that can be continued for all time as measure-valued solutions, in the case of radially symmetric monotone decreasing data for $2 - n \le \gamma < 2$. The monotonicity property is preserved for this range of γ, a feature observed in our numerical simulations but not proved rigorously until this new work. It would be interesting to examine the initial blowup profile for these more singular kernels $K(x) = |x|^\gamma/\gamma$ in the range $2 - n < \gamma < 0$ for which no numerical results currently exist.

Acknowledgments. The majority of this work was carried out as part of the PhD thesis [20] of the first author under the direction of the second author. The research was supported by NSF grant DMS-0907931. The authors would like to thank Tom Witelski and anonymous referees for their careful reading and insightful comments.

REFERENCES

[1] L. Ambrosio, N. Gigli, and G. Savaré. Gradient Flows in Metric Spaces and in the Space of Probability Measures. Lectures in Mathematics ETH Zürich. Birkhäuser Verlag, Basel, second edition, 2008.

[2] D. G. Aronson and J. L. Vázquez. *Anomalous exponents in nonlinear diffusion*, *J. Nonlinear Sci.*, 5(1):29–56, 1995.

[3] D. Benedetto, E. Caglioti, and M. Pulvirenti. *A kinetic equation for granular media*, *RAIRO Modél. Math. Anal. Numér.*, 31(5):615–641, 1997.

[4] A. L. Bertozzi and J. Brandman. *Finite-time blow-up of L^∞-weak solutions of an aggregation equation*, *Commun. Math. Sci.*, 8(1):45–65, 2010.

[5] A. L. Bertozzi, J. A. Carrillo, and T. Laurent. *Blow-up in multidimensional aggregation equations with mildly singular interaction kernels*, *Nonlinearity*, 22(3):683–710, 2009.

[6] A. L. Bertozzi, J. B. Garnett, and T. Laurent. *Characterization of radially symmetric finite time blowup in multidimensional aggregation equations*, preprint, 2011.

[7] A. L. Bertozzi and T. Laurent. *Finite-time blow-up of solutions of an aggregation equation in $\mathbf{R}^n$*, *Comm. Math. Phys.*, 274(3):717–735, 2007.

[8] A. L. Bertozzi, T. Laurent, and J. Rosado. *L^p theory for the multidimensional aggregation equation*, *Comm. Pur. Appl. Math.*, 64(1):45–83, 2011.

[9] M. Bodnar and J. J. L. Velazquez. *An integro-differential equation arising as a limit of individual cell-based models*, *J. Differential Equations*, 222(2):341–380, 2006.

[10] M. Burger, V. Capasso, and D. Morale. *On an aggregation model with long and short range interactions*, *Nonlinear Anal. Real World Appl.*, 8(3):939–958, 2007.

[11] M. Burger and M. Di Francesco. *Large time behavior of nonlocal aggregation models with nonlinear diffusion*, *Networks and Heterogeneous Media (NHM)*, 3(4):749 – 785, 2008.

[12] E. Caglioti and C. Villani. *Homogeneous cooling states are not always good approximations to granular flows*, *Arch. Ration. Mech. Anal.*, 163(4):329–343, 2002.

[13] J. A. Carrillo, M. DiFrancesco, A. Figalli, T. Laurent, and D. Slepcev. *Global-in-time weak measure solutions and finite-time aggregation for nonlocal interaction equations*, *Duke Math. J.*, 156(2):229–271, 2011.

[14] Y. L. Chuang, M. R. D'Orsogna, D. Marthaler, A. L. Bertozzi, and L. S. Chayes. *State transitions and the continuum limit for a 2D interacting, self-propelled particle system*, *Phys. D*, 232(1):33–47, 2007.

[15] H. Dong. *The aggregation equation with power-law kernels: ill-posedness, mass concentration and similarity solutions*, *Communications in Mathematical Physics*, 304(3):649–664, 2011.

[16] M. R. D'Orsogna, YL Chuang, A. L. Bertozzi, and Lincoln S. Chayes. *Self-propelled particles with soft-core interactions: patterns, stability and collapse*, *Phys. Rev. Lett.*, 96(2006), article 104302.

[17] J. Eggers and M. A. Fontelos. *The role of self-similarity in singularities of partial differential equations*, *Nonlinearity*, 22(1):R1–R44, 2009.

[18] D. D. Holm and V. Putkaradze. *Aggregation of finite-size particles with variable mobility*, *Phys Rev Lett*, 95(2005), article 226106.

[19] D. D. Holm and V. Putkaradze. *Formation of clumps and patches in self-aggregation of finite-size particles*, *Phys. D*, 220(2):183–196, 2006.

[20] Y. Huang. "Self-Similar Blowup Solutions of the Aggregation Equation". PhD thesis, University of California Los Angeles, 2010. available online as UCLA CAM Report 10-66.

[21] Y. Huang and A. L. Bertozzi. *Self-similar blowup solutions to an aggregation equation in R^n*. *SIAM J. Appl. Math.*, 70(7):2582–2603, 2010.

[22] Y. Huang, T. Witelski, and A. L. Bertozzi. *Anomalous exponents of self-similar blowup solution to an aggregation equation in odd dimensions*, preprint, 2010.

[23] E. F. Keller and L. A. Segel. *Initiation of slime mold aggregation viewed as an instability*, *J. Theor. Biol.*, 26:399–415, 1970.

[24] T. Laurent. *Local and global existence for an aggregation equation*, *Comm. Partial Differential Equations*, 32(10-12):1941–1964, 2007.

[25] H. Li and G. Toscani. *Long-time asymptotics of kinetic models of granular flows*, *Arch. Ration. Mech. Anal.*, 172(3):407–428, 2004.

[26] A. Mogilner and L. Edelstein-Keshet. *A non-local model for a swarm*, *J. Math. Biol.*, 38(6):534–570, 1999.

[27] A. Mogilner, L. Edelstein-Keshet, L. Bent, and A. Spiros. *Mutual interactions, potentials, and individual distance in a social aggregation*, *J. Math. Biol.*, 47:353–389, 2003.

[28] D. Morale, V. Capasso, and K. Oelschläger. *An interacting particle system modelling aggregation behavior: from individuals to populations*, *J. Math. Biol.*, 50(1):49–66, 2005.

[29] C. M. Topaz, A. J. Bernoff, S. Logan, and W. Toolson. *A model for rolling swarms of locusts*, *The European Physical Journal - Special Topics*, 157:93–109, 2008. 10.1140/epjst/e2008-00633-y.

[30] C. M. Topaz and A. L. Bertozzi. *Swarming patterns in a two-dimensional kinematic model for biological groups*, *SIAM J. Appl. Math.*, 65(1):152–174 (electronic), 2004.

[31] C. M. Topaz, A. L. Bertozzi, and M. A. Lewis. *A nonlocal continuum model for biological aggregation*, *Bull. Math. Biol.*, 68(7):1601–1623, 2006.

[32] G. Toscani. *One-dimensional kinetic models of granular flows*, *M2AN Math. Model. Numer. Anal.*, 34(6):1277–1291, 2000.

[33] C. Villani. Topics in Optimal Transportation, volume 58 of *Graduate Studies in Mathematics.* American Mathematical Society, Providence, RI, 2003.

Received January 2011; revised August 2011.

E-mail address: yha82@sfu.ca
E-mail address: bertozzi@math.ucla.edu